J Nanostruct 13(3): 673-684, Summer 2023

RESEARCH PAPER

Synthesis of TiO_2 Nanoparticles Using Spin-Coating and Drop-Casting Techniques for Antibacterial Application

Aseel J. Rahma [1], Hind F. Oleiwi [2], band Haider A. Abbas [3]*

[1] *Middle Technical University, Engineering Technical College, Fuel and Energy Department, Baghdad, Iraq*

[2] *Department of Physics, College of Science for Women, University of Baghdad, Iraq*

[3] *Department of postgraduate Affairs, University of Baghdad, Baghdad, Iraq*

ARTICLE INFO

Article History:
Received 19 March 2023
Accepted 27 May 2023
Published 01 July 2023

Keywords:
AFM
Drop-casting
Spin-coating
Nanoparticles
TiO_2

ABSTRACT

The "drop casting" and "spin-coating" techniques are frequently utilized to manufacture nanostructure materials like TiO_2, in which the modifying layer comprises nanoparticles (NPs). The study aims to use spin-coating and drop-casting techniques to deposit highly uniform and good adhesion nanoparticles. TiO_2 NPs have been successfully deposited using the spin-coating technique which has smoother films with discernible crystallinity used for antibacterial activity. The structural, morphological, and optical properties of TiO_2 NPs prepared through drop-casting and spin-coating techniques were studied using XRD, SEM, AFM, and UV-Vis, respectively. XRD patterns of TiO_2 NPs which were prepared by drop-casting and spin-coating techniques and the solution prepared with concentrations of (60,120) g/L was the monoclinic phase of TiO_2 nanoparticle. The average crystalline size was increased with increasing concentrations. The films have a smooth surface, a high density, and excellent adhesion to the glass substrate, according to SEM and AFM's observation of the images. Additionally, because of the growth in particle size and increasing solution concentrations, the surface roughness for synthesized samples increased. UV-Vis illustrated the allowed direct electronic transition and the value of band gaps increased with increasing concentrations of TiO_2 NPs. Finally, all the modification characterizations via the spin-coating technique contribute to knowing the effect of TiO_2 NPs concentrations on the antimicrobial activity which was increased with increasing NPs concentration.

How to cite this article
Rahma A. J., Oleiwi H. F., Abbas H.A. Synthesis of TiO_2 Nanoparticles Using Spin-Coating and Drop-Casting Techniques for Antibacterial Application. J Nanostruct, 2023; 13(3):673-684. DOI: 10.22052/JNS.2023.03.008

INTRODUCTION

Titanium dioxide (TiO_2) is a very well-known and well-researched material due to the stability of its chemical structure, biocompatibility, and physical, optical, and electrical properties like white noncombustible and odorless powder with a molecular weight of 79.9 g/mol, boiling point of 2972°C, melting point of 1843°C, and relative density of 4.26 g/cm3 at 25°C. TiO_2 is a poorly soluble particulate that has been widely used as a white pigment [1]. It has an optical and electrical properties like a highly refractive index, optical band gap of around 3.69 ± 0.10 eV, and exhibits blue shift with respect to the bulk anatase. TiO_2

* *Corresponding Author Email: aseel.jabbar@mtu.edu.iq*

exists in three mineral forms: anatase, Rutile, and Brookite [2]. The Rutile type has a tetragonal crystal structure (with prismatic habit) and exhibits a sufficient light scattering effect without absorption virtually. With a dipyramidal habit and a crystalline structure that corresponds to the tetragonal system, the anatase type is typically employed as a photocatalyst when exposed to UV light [3, 4]. As a semiconductor, it has a somewhat smaller energy band gap (3.06eV) than anatase (3.23eV). The energy band gap (~3.06eV), as a semiconductor, is slightly lower than anatase (~3.23eV) [5]. This particular TiO_2 is mostly utilized as a white paint pigment. Brookite type has an orthorhombic crystalline structure [6]. TiO_2 is often favored in the anatase form because of its high photocatalytic activity, higher specific area, non-toxicity, photochemical stability, and relative affordability. It also has a stronger negative conduction band edge potential (higher potential energy of photogenerated electrons) [7]. Today, more than four million tons of TiO_2 are manufactured annually, and this chemical is used in a variety of common products [8]. Fig. 1 illustrates an excipient used in the pharmaceutical business for the creation of sunscreen in the cosmetics sector as a colorant in white plastics and as a reasonably priced and nontoxic food pigment authorized by the appropriate European Union authorities for food additive safety [9]. In the past 10 years, researchers in the fields of physics, chemistry, and engineering have been more interested in the development of self-organized nanostructures and nanopatterns, which have a wide range of potential uses. The fundamental benefit of these procedures is that they can serve as examples of "smart" nanotechnology. It follows that it is not unexpected that a significant portion of modern materials research is focused on these nano-scale manufacturing methods. [10]. Given the significance of these two techniques for producing NPs, a comparison of their structural, morphological, and optical characteristics has been conducted. Nanostructures material has been created in recent years using a range of synthesis techniques, including hydrothermal and solvothermal [3, 11], direct oxidation method [12], chemical vapor deposition (CVD), and chemical precipitation [13], green synthesize [14], electrodeposition [15], microwave [16], drop-casting [17],and spin-coating method [18]. Utilizing drop-casting and spin-coating, two supposedly "wet" techniques that are extremely comparable. In the first process, a spin-coater is required; in the second, it is not. Both techniques are well-known and straightforward and both instances employed the same solvent. The morphological and structural characteristics of the resultant thin films, however, unambiguously define them. Thin films are produced via the widely used, simple, and affordable drop-casting technique. Additionally, the films have simply adhered to corning glass substrates without the need for a binder. The easy drop-casting method is also a potential choice for large-area thin film deposition for technological applications [19]. The versatile sol-gel technology is used to create a range of ceramic materials. In a typical sol-gel process, the precursors, which are frequently inorganic metal salts or metal organic compounds like metal alkoxides, are hydrolyzed and polymerized to produce a colloidal suspension or solution [20]. The phase change from liquid sol

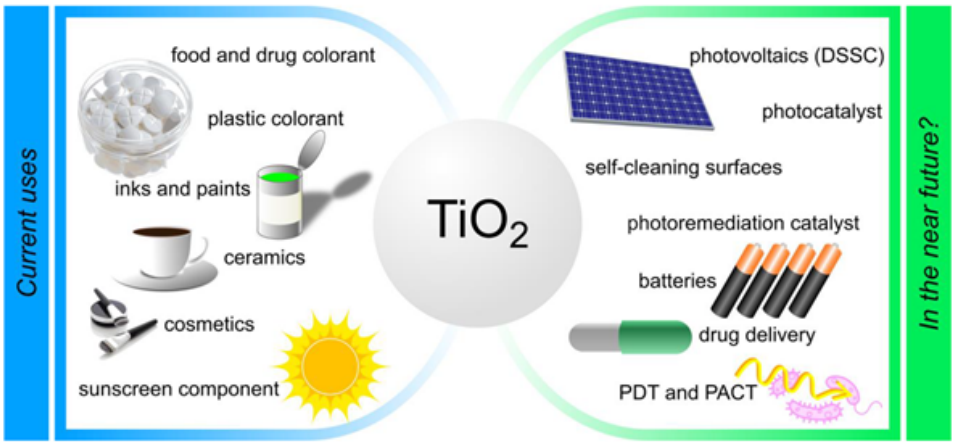

Fig. 1. Various applications of titanium dioxide/titanium dioxide nanoparticles (TiO_2/TiO_2 NPs)

to solid gel is caused by complete polymerization and solvent loss. Spin coating or dip coating are two methods that may be used to create thin coatings on a substrate. When the solution is poured into a mold, a wet gel will develop, and after additional drying and heating, the wet gel will harden into a thick ceramic. If the solvent in a wet gel is extracted under a supercritical state, a very porous and low-density substance known as an aerogel is created [21]. The spin coating process is one of the main methods for depositing material layers onto the flat surface of the substrate. This method's foundation is the dispersion of a solution onto the substrates and anchoring it to them, which accounts for how simple it is. The turntable of this contraption was rotating at thousands of revolutions per minute under the control of the central force. The substrate is dried using this instrument [22].This study focuses on preparation TiO_2 NPs using different concentrations and two different techniques (spin coating and drop-casting). In addition, study the influence of the concentration and preparing methods on the TiO_2NPs properties and examined the performance structure as antibacterial activity.

MATERIALS AND METHODS

Materials

The materials used in this study include chemical materials like P-25 TiO_2 powder (DIREVO Industrial Biotech, Germany). Ethanol (Eth) (99% of purity, Brazil), Deionized distilled water (University of Baghdad, Conductivity 10 µs/cm), Glass substrate (Alfa Aesar A Johnson Matthey company.

Sample preparation

Cleaning the substrate is the first crucial step in creating an effective thin film. Before the deposition process, the soda Lima glass (20 mm× 20 mm ×2 mm) was ultrasonically cleaned in acetone and subsequently with 2-propanol for 20 min, and then rinsed with deionized water. The appropriate TiO_2 concentration required to produce a homogenous coating on the substrate was determined depending on the literature review and used two different concentrations (60 and 120 g/L). TiO_2 solutions with different concentrations were created by mixing P-25 TiO_2 powder with 200 mL of ethanol. The mixtures were aggressively churned until uniform and white in color.

Drop-Casting

The cleaned soda lime glass was carefully coated with each produced TiO_2 nanoparticle (TiO_2NPs) solution for 30 seconds (Fig. 2). The residual solvent was removed by heated the substrates at 100℃ for 10 min using the hot-plate device to evaporate all residual solvent and repeated this process three times. At this stage, TiO_2NPs was obtained by annealed these substrates inside the furnace for one hour at 300℃. TiO_2NPs may be made easily and affordably by drop casting, the dispersion volume and concentration have an impact on the film's thickness and other characteristics as well. The film structure is influenced by the substrate's wetness, the velocity of evaporation, and the drying procedure. This method has a number of drawbacks, including difficulty controlling film thickness and non-uniform film formation on large wafers [23].

Spin-Coating

P-25 TiO_2 powder was combined with 200

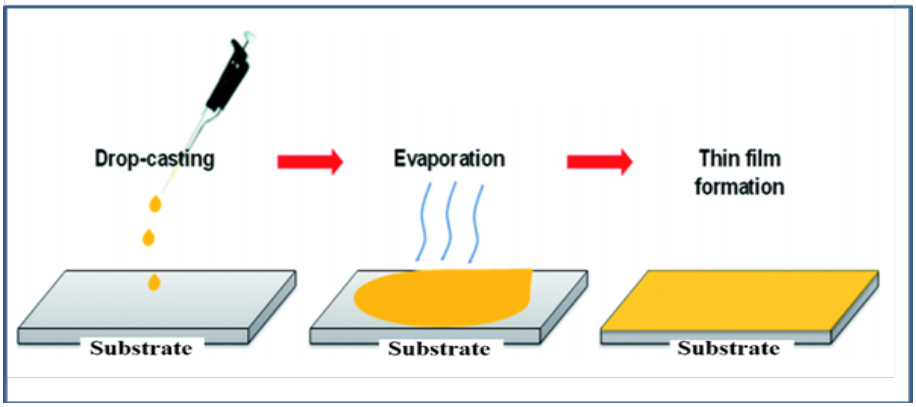

Fig. 2. Drop-Casting technique

mL of ethanol to create TiO_2 solutions with concentrations of 60 and 120 g/L, respectively. The mixtures were aggressively churned until uniform and white in color. Each prepared TiO_2 nanoparticle solution was carefully deposited onto the cleaned soda lime glass (20 mm × 20 mm × 2 mm) for the ideal coating time (30 seconds at 3000 rpm). After each coating process a heating process at 100 ºC for 15 min. Then, the coated glass substrates were annealed. These processes have a number of benefits, including large scale, low temperature production processing, and the use of a wide range of substrates, a wide range of structural dimensions, minimal material waste, and cheap cost [24].

Activation and preparation of the Bacterial isolates

The bacterial isolates used in this study were obtained from the Central Environmental Laboratory/College of Science/ University of Mustansiriya; it was gram-positive Bacteria (*Staphylococcus*. *Aureus*, *Staphylococcus epidermidis*) and Gram-negative bacteria (*Pseudomonas. Klebsiella, Streptococcus sp*.). To assess the infection antibacterial activity and fungal type (Candida) to assess the infection antifungal activity of these as-prepared NPs. Lines of bacterial isolates were placed on brain heart infusion agar and incubated for 18 hours at 37°C. One colony was then picked from the media plate and inoculated in 5 ml of brain heart infusion broth and then incubated overnight at 37°C. Fig 5 shows the antibacterial samples at these conditions.

Characterization

The prepared samples were analyzed using a variety of methods. The first technique employed an X-ray diffraction system with a Cu-Ka x-ray tube as the target and a power diffraction system with a wavelength of 1.5406 A to observe the crystal structure and identify the phase of the samples produced. The scan mode is continuous with a speed of 5.0000 degrees per minute, the voltage and current are 40 KV, 30 mA respectively. Atomic force microscopy type (AA3000) was used to examine the sample surface topography, to determine the grain size of agglomerations on the surface and roughness for TiO_2 NPs prepared on glass substrates by two different method (drop-casting and spin-coating). This technique provides information regarding sample surface roughness at the nanoscale scale. UV-Visible region were recorded using spectrophotometer (SHIMADZU UV- 1650 PC).

RESULTS AND DISCUSSION

Surface coating uniformity is an important criterion in the present study. The optimal TiO_2 concentration required to produce a uniform coating on the substrate was identified by depositing two different concentrations using two different methods of TiO_2NPs on glass substrates and by analyzing the properties of the TiO_2-coated substrates. Analytical results indicated that the optimal TiO_2NPs concentration is 120.0 g/L for two methods. Fig. 4 shows glass substrates coated with different TiO_2NPs concentrations images of these samples. As shown in these images, the surfaces of the substrates coated with 60.0 g/L TiO_2 appear rough and uneven and the roughness of the coating surface decreases as TiO_2 concentration increases.

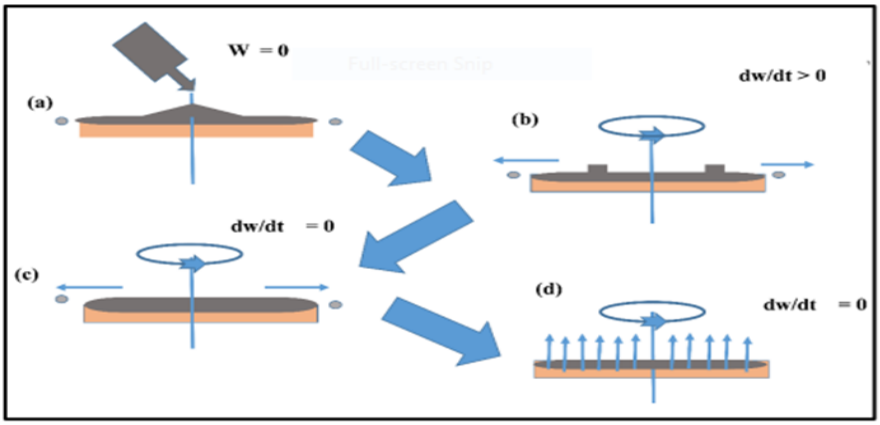

Fig. 3. Spin coating technique with four stages

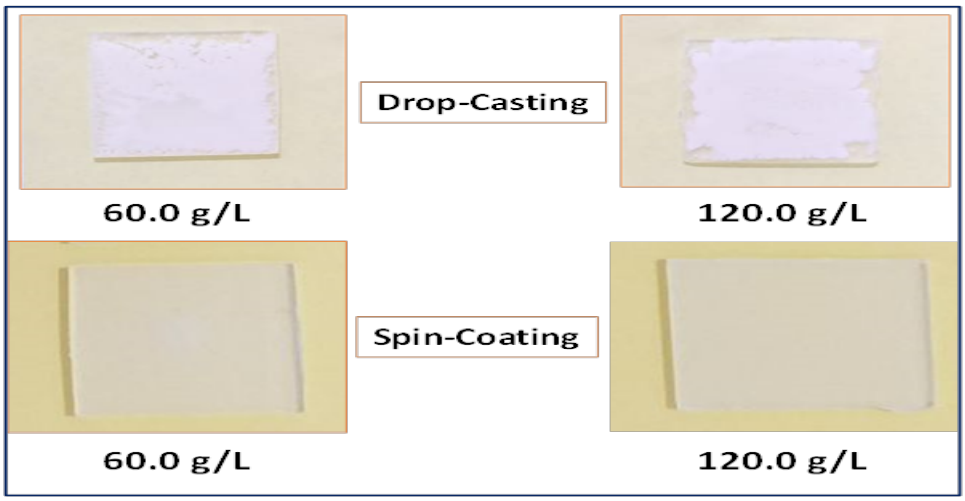

Fig. 4. Images of glass surface coated with TiO_2 at two solution concentrations

Fig. 5 shows the XRD patterns of TiO_2NPs which prepared by drop-casting technique and the solution prepared with concentrations of (60 and 120 g/L). The anatase phase of TiO_2 is represented by all sharp peaks observed in the XRD patterns. There are noticeable diffraction peaks located at 2θ= 25.35°, 37.90°, 48.10° , 54.49° and 62.92º which is observed on the spectra of drop-casting process attribute to (101), (004), (200), (105) and (204) orientation plane of anatase-TiO_2. These results indicate that the synthesized powders in monoclinic phase of TiO_2 nanoparticle can be obtained by double-step drop-casting process and agreed well with (JCPDS card number 01-084-1285). These results are nearly in agreement with research [25]. The well-known Scherrer's formula, expressed in Eq.1, can be used to calculate the average crystallite size of TiO_2 from the full-width at half maximum (FWHM).

$$D = K\lambda / \beta \cos\theta \quad (1)$$

where D is the crystallite size, K is the form factor, λ is the X-ray wavelength of Cu Ka (0.154 nm), β is the full-width at half maximum (FWHM), and θ is the Bragg angle. Fig. 5 illustrates the results of calculating the crystallite size of TiO_2 produced by the drop-casting procedure using the (101) plane diffraction peak. The average crystallite size were increased from 6.31nm to 8.01nm for 60g/L and 120g/L, respectively. It noticed that the crystallite size of the prepared samples are increased by

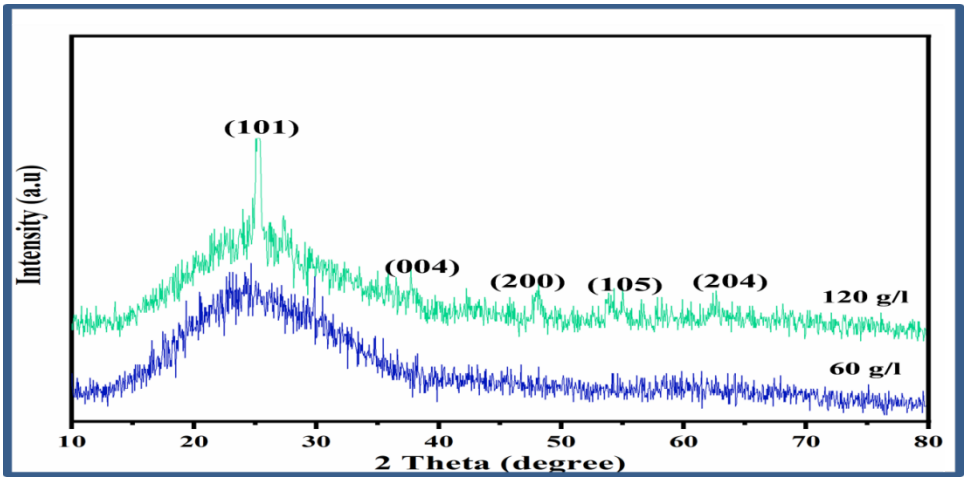

Fig. 5. The XRD pattern of the synthesized TiO_2NPs via drop-casting method

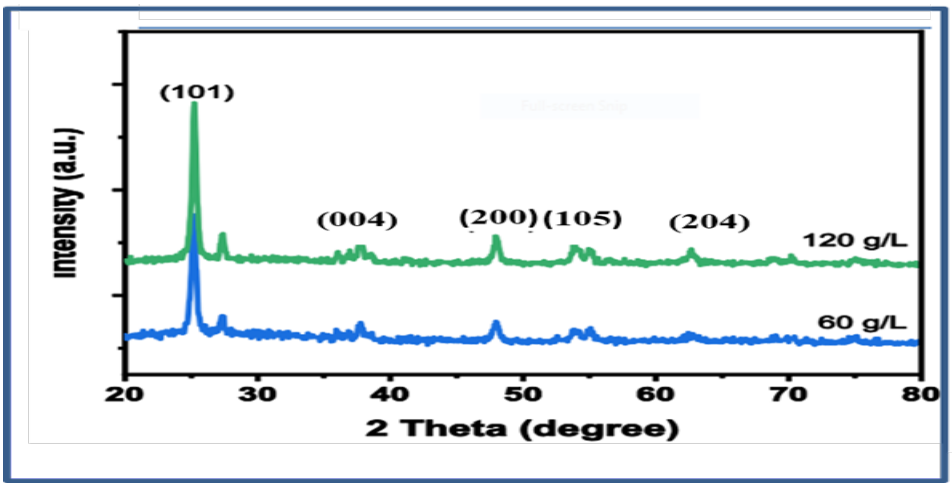

Fig. 6. The XRD pattern of the synthesized TiO_2NPs via spin-coating method

increasing the TiO_2 concentration and a good agreement with research [26].

Fig. 6 explains the phase composition and the crystalline size of the two samples that prepared by spin-coating technique and the solution prepared with concentrations (60, 120 g/L) in the 2θ range from 20º to 80º. The anatase phase of TiO_2NPs is represented by all sharp peaks observed in the XRD patterns. Five peaks were identified in the anatase phase detected around 2θ values of 25.20°, 37.78°, 48.08°,54.66° and 63.01º which is observed on the spectra of spin coating process attribute to (101), (004), (200), (105) and (204) orientation plane, respectively. These findings indicate that spin coating can be used to obtain powders of TiO_2NPs in the monoclinic phase, which agrees well with previous findings (JCPDS card number 01-084-1285).The average crystallite

Table 1. The structure properties of TiO_2NPs prepared by drop-casting and spin-coating approaches

Sample	Concentration (g/L)	2θ (Deg.)	d_{hkl} (A°)	FWHM (Deg.)	hkl	C.S. (nm)	Average C.S. (nm)	Phase
TiO_2 (drop-casting)	60	25.357	3.0472	1.2899	(101)	6.16304	6.31	Anatase
		37.902	2.6286	1.20121	(004)	6.6197		
		48.103	1.8188	2.90319	(200)	5.9487		
		54.496	1.596	1.2519	(105)	10.825		
		62.922	1.4822	3.92117	(204)	2.0343		
	120	25.375	3.1272	0.9899	(101)	8.030	8.01	Anatase
		37.902	2.7186	1.2012	(004)	6.619		
		48.103	1.9088	2.9031	(200)	5.948		
		54.496	1.6259	1.2519	(105)	10.825		
		62.922	1.5648	0.9211	(204)	8.659		
TiO_2 (spin-coating)	60	25.2	3.1227	0.9468	(101)	8.396	9.78	Anatase
		37.78	2.7276	1.0221	(004)	7.779		
		48.08	1.8188	1.1329	(200)	12.99		
		54.66	1.5359	1.2319	(105)	11.00		
		63.01	1.6648	0.9117	(204)	8.749		
	120	25.2	3.2527	0.4846	(101)	16.401	10.84	Anatase
		37.78	2.7127	1.1120	(004)	7.150		
		48.08	1.8928	2.0319	(200)	8.499		
		54.66	1.5129	1.0231	(105)	13.244		
		63.01	1.6568	0.8911	(204)	8.950		

size of TiO_2 can be calculated from the Eq.(1) above and increased from 9.78nm to 10.84nm for 60 and 120g/L, respectively, and this is a good agreement to researches [26, 27]. Drop-casting and spin-coating methods have been used to successfully prepare TiO_2 nanoparticle, Top-view FESEM images of TiO_2 with 200 nm scales are shown in Fig. 7 and 8, respectively. The critical roles of preparing method in changing the fundamental characteristics of TiO_2 and its antibacterial activity were examined in detail. According to FESEM images which were analyzed using Image J software, TiO_2 was uniformly distributed on FTO substrate. Additionally, the figures also display the TiO_2 crystalline that forms has a smooth surface and no agglomeration had developed there.

Figs. 9 (a and b) show the AFM images and the chart of grain density distribution of the TiO_2 NPs films at varying solution concentrations (60 and 120 g/L) via drop-casting method. The substrate surface is well covered with grains that are almost consistently dispersed throughout it, according to AFM scans, which also demonstrate that the films are homogenous. The nanocrystalline (TiO_2) grains are visible in the surface morphology, and when the concentration is raised, they mix to produce noticeably denser films. From the images, it is observed that the films consist of grain size 55.05nm and 62.037 nm for 60 g/L and 120 g/L, respectively. The films' surfaces have some degree of roughness to them. Additional information on the surface morphology of thin films is provided by the surface roughness. In optical coatings, the variation in surface roughness of thin films is significant. It impacts the optical characteristics of thin films and increases optical absorption. These results are nearly in agreement with research [28]. Fig. 10 shows the AFM images of the TiO_2 NPs films at two different solution concentrations 60 and 120 g/L. The photos clearly show that the films

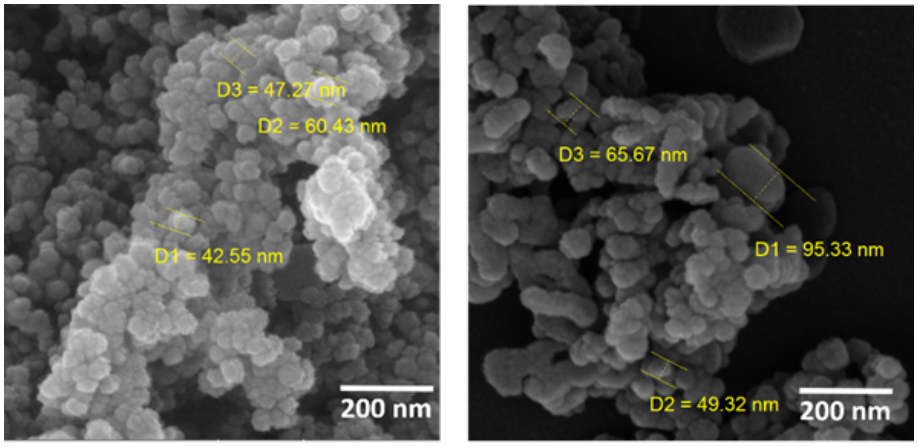

Fig. 7. FESEM images of the synthesized TiO_2NPs via drop-casting method

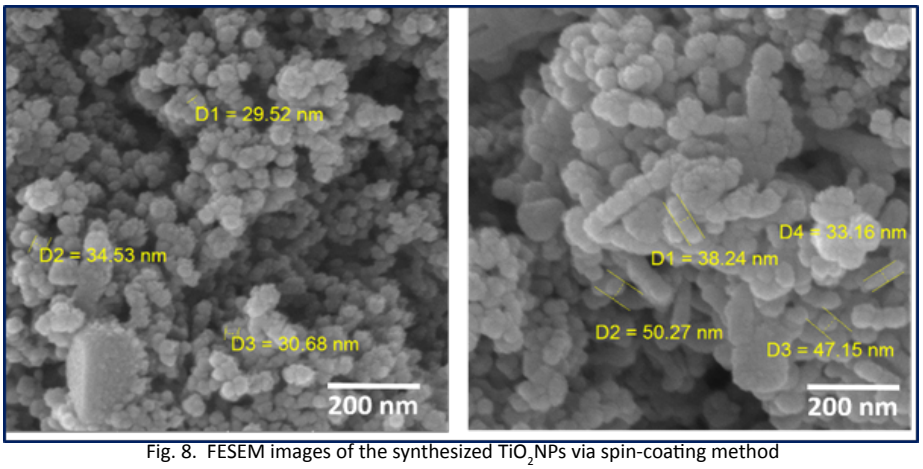

Fig. 8. FESEM images of the synthesized TiO_2NPs via spin-coating method

have a smooth surface, a high density, and good adhesion to the glass substrate. Also, the surface roughness for synthesizing samples increased with the increasing solution concentrations due to increasing particle size, which increased from 63.61nm to 72.44 nm as shown in (Table 2) when the solution concentrations increase from 60 g/L to 120 g/L. The diameter distribution of the samples demonstrated that the average particle size increased with increasing solution concentrations, which might be attributed to an increase in film crystallanity [29]. This results agrees well with the XRD results.

The optical band gap for the TiO_2 films that prepared by drop-casting method was determined by extrapolating the linear portion of $(\alpha h\upsilon)^2$ versus photon energy ($h\upsilon$) at $\alpha h\upsilon=0$, then the intercept with x-axis at $\alpha h\upsilon=0$, give the value of Eg. The energy gap can be calculated from Eq. 2:

$$\alpha h\nu \propto (h\nu - \mathrm{Eg})^2 \quad (2)$$

As shown in Fig. 10 which illustrate the allowed direct electronic transition. The value of band gaps increased from 2.5 eV to 2.87 eV for (60,120) g/L, respectively. Since the film thickness increased significantly with concentration, the thickness dependence of the band gap can be referred to

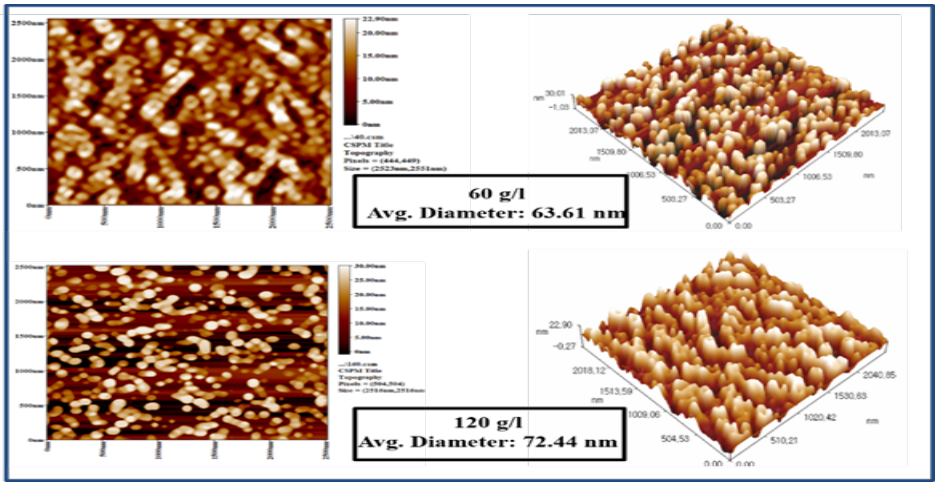

Fig. 9. Atomic force microscopy of the synthesized TiO_2 nanoparticles using drop-casting technique at two solution concentrations.

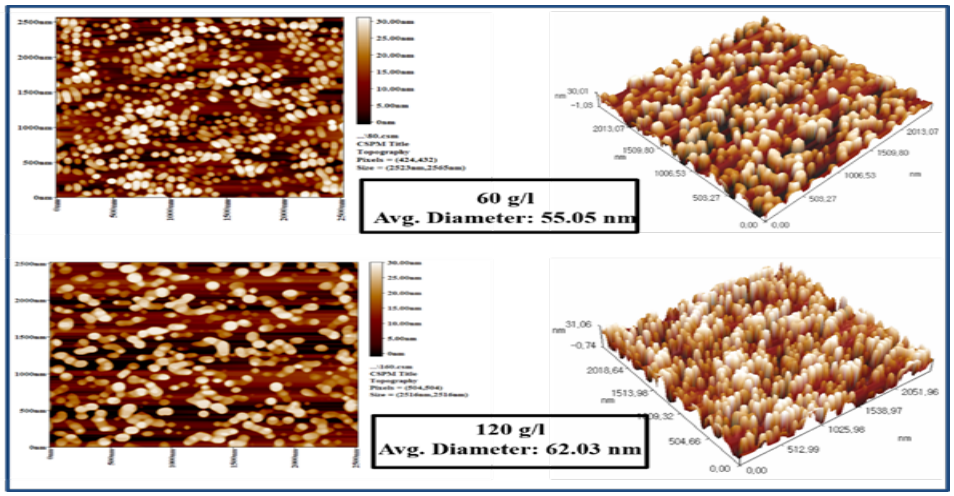

Fig. 10. Atomic force microscopy of the synthesized TiO_2 nanoparticles using spin-coating technique at two solution concentrations.

Table 2. Average diameter of TiO_2 nanoparticles preparing via two different technique (Drop-casting and Spin-coating) at two different solution concentrations

Technique	Solution Concentration (g/L)	Average Roughness (nm)	Average Diameter (nm)	Root Mean Square (nm)
Drop-casting	60	7.74	55.05	8.93
	120	7.94	62.037	9.16
Spin-Coating	60	4.74	63.61	5.7
	120	4.99	72.44	5.76

as I an increase in barrier in polycrystalline films according to change in grain size, since when the grain size increases the wideness of the electronic levels and the band gap increases. This is because the pairings of electron hole pairs are significantly closer to one another, making it impossible to ignore their Columbic contact, resulting in a larger total kinetic energy. Reduced strain and density of dislocations [28]. At the same way noticed the band gap will be increased with increasing the concentration of TiO_2 NPs which prepared by spin-coating technique as seen in Fig. 12, and this results were a good agreement to research [30].

Antibacterial Activity of the TiO_2 Nanoparticles (NPs)

The antibacterial activity of TiO_2 NPs was studied using agar-well diffusion method against each of the previously mentioned microorganisms. The tested bacteria were uniformly flushed onto Muller-Hinton agar plates using a sterile cotton swab, then for 6 mm diameter wells were made using a sterile well drill. Freshly synthesized TiO_2 NPs solutions of (60 and 120) g/L concentrations were added to the corresponding wells. The samples were then incubated overnight at 37 °C. After the incubation period, the region of inhibition (in mm diameter) was observed and tabulated as shown in Fig. 13. After the incubation period, positive test results were recorded when an area of inhibition (in mm diameter) was observed around the well as shown in (Table3). TiO_2 NPs prepared using a spin-coting process exhibited high antibacterials activity against gram-positive Bacteria (*Staphylococcus*. *Aureus*, *Staphylococcus epidermidis*), Gram-negative bacteria (*Pseudomonas. Klebsiella, Streptococcus sp.),* and

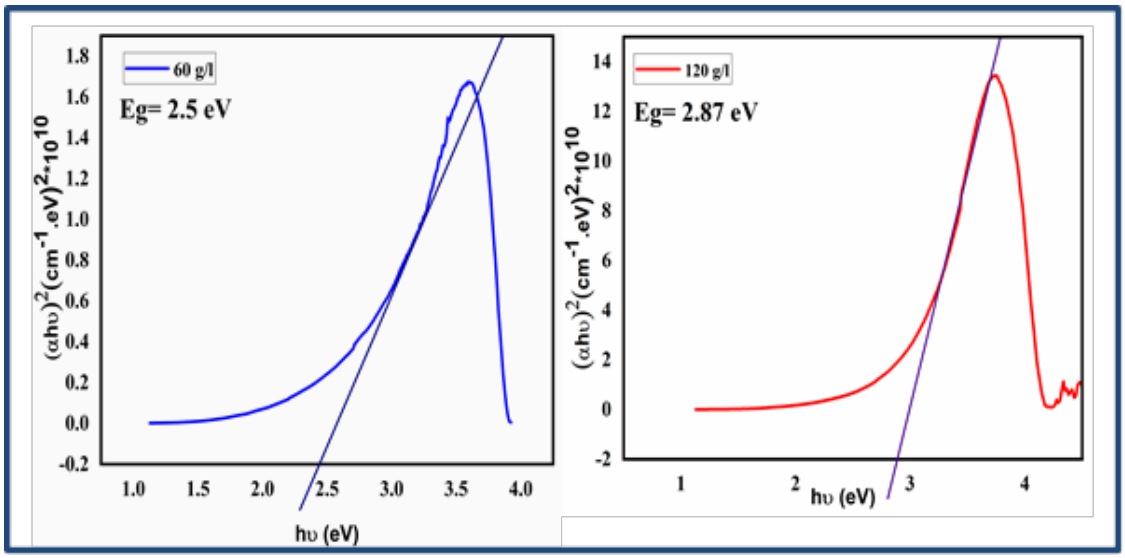

Fig. 11. The variation of $(\alpha h\upsilon)^2$ versus photon energy of the synthesized TiO_2 nanoparticles prepared by drop-casting at two solution concentrations.

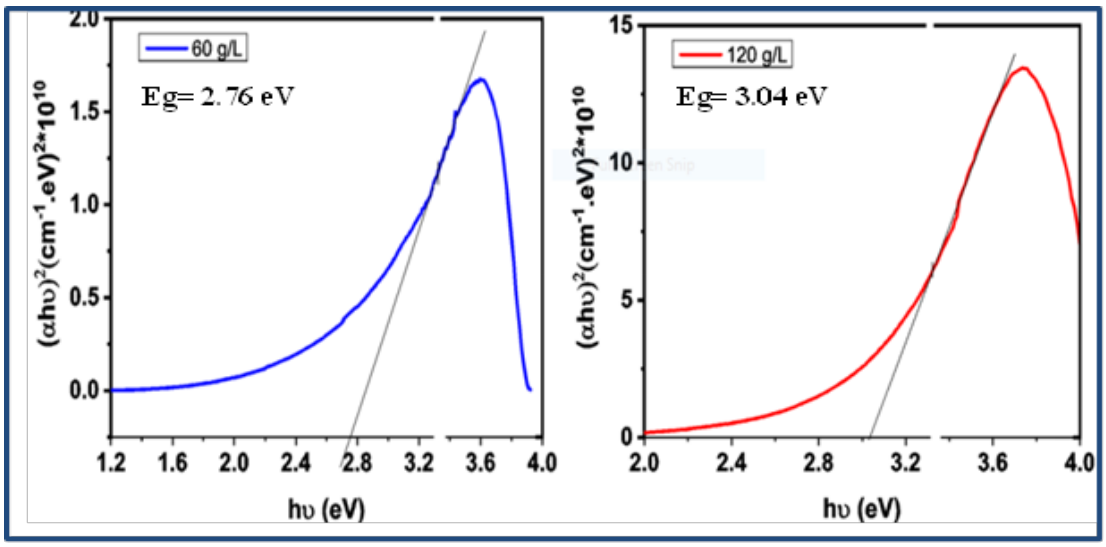

Fig. 12. The variation of $(\alpha h\upsilon)^2$ versus photon energy of the synthesized TiO_2 nanoparticles prepared by spin-coating at two solution concentrations.

fungal type (Candida) for both concentrations 60 g/L and 120 g/L. The maximum inhibition zone for gram-positive Bacteria (Klebsiella. pneumonia) at 60 g/L TiO2 NPs, while 120 g/L TiO2 NPs showed the maximum inhibition zone for gram-positive Bacteria (Klebsiella. pneumonia) and gram-negative Bacteria (E. coli). TiO_2 NPs (60 g/L) show excellent antibacterial activity against Gram-positive (*Klebsiella. Pneumonia* with inhabition zone 10 mm) than Gram-negative bacteria (*E. coli* with inhabition zone 6 mm). When opposed to Gram-positive bacteria, Gram-negative bacteria have a considerably thinner peptidoglycan coating, which plays a critical function in preserving cell integrity. Gram-negative bacteria have more complex cell walls than Gram-positive bacteria, which acts as a diffusion barrier and makes them less vulnerable to antibacterial agents [31].

CONCLUSION

On glass substrates, TiO_2 thin films were created using the drop-casting and spin-coating techniques. As a function of the concentration, the structural,

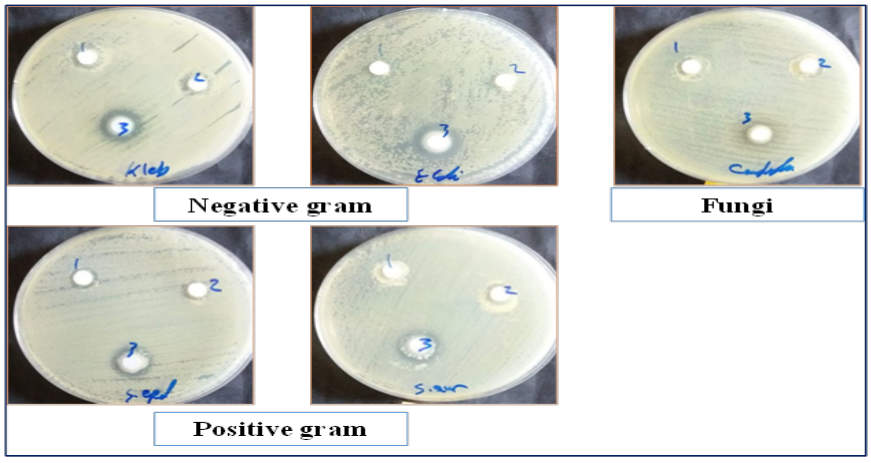

Fig. 13. Antibacterial activity of the synthesized TiO_2 nanoparticles prepared by spin-coating at two concentrations

Table 3. Zone of inhibition (mm) of A. hydrophila synthesized TiO_2 nanoparticles against various microorganisms.

Microorganisms	Diameter of inhibition zone (mm)	
	60 g/L Mean	120 g/L Mean
Staphylococcus. aureus	6	10
Staphylococcus. epidermidis)	8	13
E. coli	6	15
Klebsiella. pneumonia	10	15
candida	6	9

morphological, and optical characteristics of the films were investigated. The TiO_2 films' XRD patterns demonstrate that a single-phase with an anatase crystal structure exists. A (101) major peak can be seen in the XRD patterns, which is caused by TiO_2 crystals that are growing along the c-axis. As the TiO_2 nanoparticle concentration rose, the crystallite size also increased. According to AFM pictures, the density of the films rises when the concentration is increased. The films' morphological characteristics demonstrate. The films' surfaces have some degree of roughness to them. Band gap grew at both ways (drop-casting) as concentration increased.

ACKNOWLEDGEMENTS

Special thanks to the staff of Laboratory of Chemistry and Physics in University of Baghdad.

CONFLICT OF INTEREST

The authors declare that there is no conflict of interests regarding the publication of this manuscript.

REFERENCE

1. Bakri AS, Sahdan MZ, Adriyanto F, Raship NA, Said NDM, Abdullah SA, et al. Effect of annealing temperature of titanium dioxide thin films on structural and electrical properties. AIP Conf Proc: Author(s); 2017.
2. Daβler A, Feltz A, Jung J, Ludwig W, Kaisersberger E. Characterization of rutile and anatase powders by thermal analysis. J Therm Anal. 1988;33(3):803-809.
3. Byranvand MM, Kharat AN. One pot green synthesis of gold nanowires using pomegranate juice. Mater Lett. 2014;134:64-66.
4. Macwan DP, Dave PN, Chaturvedi S. A review on nano-TiO2 sol–gel type syntheses and its applications. Journal of Materials Science. 2011;46(11):3669-3686.
5. Yan EYC, Zakaria S, Chia CH. One-step synthesis of titanium oxide nanocrystal- rutile by hydrothermal method. AIP Conf Proc: AIP Publishing LLC; 2014.
6. Pauling L, Sturdivant JH. XV. The crystal structure of brookite. Zeitschrift für Kristallographie - Crystalline Materials. 1928;68(1-6):239-256.
7. Balgude SD, Barkade SS, Mardikar SP. Metal Oxides for High-Performance Hydrogen Generation by Water Splitting. Multifunctional Nanostructured Metal Oxides for Energy Harvesting and Storage Devices: CRC Press; 2020. p. 169-194.
8. Shi H, Magaye R, Castranova V, Zhao J. Titanium dioxide nanoparticles: a review of current toxicological data. Part Fibre Toxicol. 2013;10(1).
9. Khan MZ, Militký J, Wiener J, Ali A. Titanium Dioxide. Textiles and Their Use in Microbial Protection: CRC Press; 2021. p. 205-219.
10. Singh AK, Dubey K, Srivastava RK, Bahga SS. Scaling Behavior in Electrohydrodynamic Jetting of Polymeric Solutions. Volume 10: Micro- and Nano-Systems Engineering and Packaging; 2019/11/11: American Society of Mechanical Engineers; 2019.
11. Rahma AJ, Oleiwi HF, Khaleel SG, Mutter MM. Morphology, Structure, and Optical Properties of ZnO nanorods/Eosin-y Grown via Microwave-assisted Hydrothermal Method. IOP Conference Series: Materials Science and Engineering. 2021;1095(1):012007.
12. Kumar A. Different Methods Used for the Synthesis of TiO_2 Based Nanomaterials: A Review. American Journal of Nano Research and Applications. 2018;6(1):1.
13. Shaker DS, Abass NK, Ulwali RAU. Preparation and study of the Structural, Morphological and Optical properties of pure Tin Oxide Nanoparticle doped with Cu. Baghdad Science Journal. 2022;19(3):0660.
14. Hassan E, Al-saidi MH, A RJ, Thahab SM. Preparation and Characterization of ZnO Nano-Sheets Prepared by Different Depositing Methods. Iraqi Journal of Science. 2022:538-547.
15. An W-J, Thimsen E, Biswas P. Aerosol-Chemical Vapor Deposition Method For Synthesis of Nanostructured Metal Oxide Thin Films With Controlled Morphology. The Journal of Physical Chemistry Letters. 2009;1(1):249-253.
16. Pimentel A, Nunes D, Pereira S, Martins R, Fortunato E. Photocatalytic Activity of TiO_2 Nanostructured Arrays Prepared by Microwave-Assisted Solvothermal Method.

Semiconductor Photocatalysis - Materials, Mechanisms and Applications: InTech; 2016.
17. Aslan F, Esen H, Yakuphanoglu F. The effect of coumarin addition on the electrical characteristics of Al/Coumarin:CdO/p-Si/Al photodiode prepared by drop casting technique. Optik. 2019;197:163203.
18. Liaqat MA, Hussain Z, Khan Z, Akram MA, Shuja A. Effects of Ag doping on compact TiO_2 thin films synthesized via one-step sol–gel route and deposited by spin coating technique. Journal of Materials Science: Materials in Electronics. 2020;31(9):7172-7181.
19. Kaliyaraj Selva Kumar A, Zhang Y, Li D, Compton RG. A mini-review: How reliable is the drop casting technique? Electrochem Commun. 2020;121:106867.
20. Kozuka H, Kuroki H, Sakka S. Flow characteristics and spinnability of sols prepared from silicon alkoxide solution. Journal of Non-Crystalline Solids. 1988;100(1-3):226-230.
21. Gurav JL, Jung I-K, Park H-H, Kang ES, Nadargi DY. Silica Aerogel: Synthesis and Applications. Journal of Nanomaterials. 2010;2010:1-11.
22. Intelligent Transportation Systems Architectures (Artech House Intelligent Transportation Systems Library). Bob McQueen and Judy McQueen. Artech House Publishers, 685 Canton Street, Norwood, MA 02062, USA, 1999. 467 pp. + xxxiii. ISBN 0-89006-525-X. US $99.00. Transportation Research Part A: Policy and Practice. 2003;37(2):192.
23. Kajal P, Ghosh K, Powar S. Manufacturing Techniques of Perovskite Solar Cells. Applications of Solar Energy: Springer Singapore; 2017. p. 341-364.
24. Sonoda T, Fujisawa T, Fujii A, Yoshino K. Optical properties of self-assembled thin-film of poly(p-phenylene vinylene)s and its application to light-emitting devices with microring geometry. Appl Phys Lett. 2000;76(22):3227-3229.
25. Al-Inad TM, Tawfik W, Farooq WA, Aldwayyan AS. LIP characteristics of nanostructured ZnO thin films. 2013 High Capacity Optical Networks and Emerging/Enabling Technologies; 2013/12: IEEE; 2013.
26. Toghan A, Modwi A, Khairy M, Taha KK. Influence of TiO_2 concentration on the characteristics of ZnO nanoparticles fabricated via sonication assisted with gelatin. Chem Phys. 2021;551:111350.
27. Ezike SC. Effect of Concentration Variation on Optical and Structural Properties of TiO_2 Thin Films. Journal of Modern Materials. 2020;7(1):1-6.
28. Sabry RS, Al-Haidarie YK, Kudhier MA. Synthesis and photocatalytic activity of TiO_2 nanoparticles prepared by sol–gel method. J Sol-Gel Sci Technol. 2016;78(2):299-306.
29. Xing Y, Li X, Guo X, Li W, Chen J, Liu Q, et al. Effects of Different TiO2 Nanoparticles Concentrations on the Physical and Antibacterial Activities of Chitosan-Based Coating Film. Nanomaterials. 2020;10(7):1365.
30. Pal M, Pal U, Jiménez JMGY, Pérez-Rodríguez F. Effects of crystallization and dopant concentration on the emission behavior of TiO_2:Eu nanophosphors. Nanoscale Research Letters. 2012;7(1).
31. S G, Belay A, Reddy Ar C, Z B. Synthesis and Characterizations of Zinc Oxide Nanoparticles for Antibacterial Applications. Journal of Nanomedicine and Nanotechnology. 2017;s8.